Development 139, 3859-3869 (2012) doi:10.1242/dev.078550

$S1P_1$ inhibits sprouting angiogenesis during vascular development

Adi Ben Shoham[1], Guy Malkinson[2], Sharon Krief[1], Yulia Shwartz[1], Yona Ely[2], Napoleone Ferrara[3], Karina Yaniv[2] and Elazar Zelzer[1,*]

SUMMARY

Coordination between the vascular system and forming organs is essential for proper embryonic development. The vasculature expands by sprouting angiogenesis, during which tip cells form filopodia that incorporate into capillary loops. Although several molecules, such as vascular endothelial growth factor A (Vegfa), are known to induce sprouting, the mechanism that terminates this process to ensure neovessel stability is still unknown. Sphingosine-1-phosphate receptor 1 ($S1P_1$) has been shown to mediate interaction between endothelial and mural cells during vascular maturation. In vitro studies have identified $S1P_1$ as a pro-angiogenic factor. Here, we show that $S1P_1$ acts as an endothelial cell (EC)-autonomous negative regulator of sprouting angiogenesis during vascular development. Severe aberrations in vessel size and excessive sprouting found in limbs of *S1P1*-null mouse embryos before vessel maturation imply a previously unknown, mural cell-independent role for $S1P_1$ as an anti-angiogenic factor. A similar phenotype observed when *S1P1* expression was blocked specifically in ECs indicates that the effect of $S1P_1$ on sprouting is EC-autonomous. Comparable vascular abnormalities in $S1p_1$ knockdown zebrafish embryos suggest cross-species evolutionary conservation of this mechanism. Finally, genetic interaction between *S1P1* and *Vegfa* suggests that these factors interplay to regulate vascular development, as Vegfa promotes sprouting whereas $S1P_1$ inhibits it to prevent excessive sprouting and fusion of neovessels. More broadly, because S1P, the ligand of $S1P_1$, is blood-borne, our findings suggest a new mode of regulation of angiogenesis, whereby blood flow closes a negative feedback loop that inhibits sprouting angiogenesis once the vascular bed is established and functional.

KEY WORDS: Sphingosine-1-phosphate receptor 1 ($S1P_1$), Endothelial cell, Mouse, Limb vasculature, Zebrafish, Angiogenesis, Vascular remodeling, Sprouting, Filopodia, Intersegmental vessels, Caudal vein plexus

INTRODUCTION

The embryonic vascular system is initiated when endothelial precursors called angioblasts form a primitive network of tubular endothelial structures in a process known as vasculogenesis (Risau, 1991). Next, the uniform primary plexus undergoes remodeling to generate a more complex, hierarchical network of vessels of varying sizes. This occurs by sprouting, branching and pruning of pre-existing vessels in a process called angiogenesis (Risau, 1997). The remodeling process is tightly coordinated in order to supply the increasing demands of the developing embryo for nutrients and oxygen.

Sprouting angiogenesis forms new vessels by creating loops between neighboring sprouts through anastomosis (reviewed by Potente et al., 2011). During this process, endothelial cells (ECs) are specified into either tip or stalk cells by lateral inhibition, through activation of the Dll4/Notch signaling pathway by vascular endothelial growth factor A (Vegfa) (Hellstrom et al., 2007; Lobov et al., 2007; Suchting et al., 2007). Tip cells are found at the edge of the sprout and lead the way by extending numerous long filopodia and migrating in response to angiogenic cues. These include Vegfa signaling, which promotes the sprouting process (Gerhardt, 2008; Gerhardt et al., 2003), and the ephrin-Eph, Slit-Robo, netrin-Unc5b and semaphorin-plexin families, which mediate tip cell guidance (Adams and Eichmann, 2010; De Smet et al., 2009; Larrivee et al., 2009; Ruhrberg et al., 2002; Weinstein, 2005). Adjacent stalk cells then proliferate towards the migrating tip cell and form the vascular lumen (Gerhardt et al., 2003).

Once a vascular network achieves adequate size and configuration, sprouting angiogenesis has to cease to allow neovessel stabilization. In contrast to the wealth of information on the mechanism that promotes angiogenesis and vessel growth, little is known on the mechanism that terminates sprouting angiogenesis to prevent excessive sprouting and stabilize the vasculature. A mechanism that was implicated in vascular stabilization is the maturation process, during which vessels are invested with mural cells, namely vascular smooth muscle cells (VSMCs) and pericytes (Benjamin et al., 1998; Carmeliet, 2000; Hungerford and Little, 1999; Jain, 2003). Mural cells provide structural support for increased blood pressure and control EC proliferation, vascular permeability and vessel diameter (Nehls and Drenckhahn, 1993). Several molecules were identified to control the recruitment of these cells to the developing vessels, including $S1P_1$ (S1pr1 – Mouse Genome Informatics) (Allende and Proia, 2002; Allende et al., 2003), a G protein-coupled receptor for sphingosin-1-phosphate (S1P; also known as Mbtps1) (Lee et al., 1998).

S1P is a bioactive sphingolipid metabolite produced by several cellular sources, such as platelets, erythrocytes and ECs (Hla et al., 2008; Pappu et al., 2007; Venkataraman et al., 2008), and is found in high concentration in the blood serum (Hla et al., 2008; Yatomi et al., 2000). The vital role of $S1P_1$ in vascular development was demonstrated by knockout of the *S1P1* gene in mice (Liu et al., 2000). *S1P1*-null embryos die in utero between E12.5 and E14.5 as

[1]Department of Molecular Genetics, Weizmann Institute of Science, Rehovot 76100, Israel. [2]Department of Biological Regulation, Weizmann Institute of Science, Rehovot 76100, Israel. [3]Genentech, South San Francisco, CA 94080, USA.

*Author for correspondence (eli.zelzer@weizmann.ac.il)

Accepted 25 July 2012

a result of severe bleeding throughout their bodies. Vasculogenesis and angiogenesis in those mice appeared normal and the vascular abnormalities were attributed to a defect in the association of mural cells with nascent vessels, which exhibited incomplete coverage by these cells (Allende and Proia, 2002; Liu et al., 2000).

Interestingly, *S1P$_1^{-/-}$* embryos also exhibit defective vasculature in the limb bud (Chae et al., 2004). Previous studies by ourselves and others have shown that the limb vasculature undergoes extensive remodeling during its development (Ambler et al., 2001; Eshkar-Oren et al., 2009; Seichert and Rychter, 1972a; Seichert and Rychter, 1972b). The primary vasculature of the limb bud originates from the dorsal aorta. During limb development, *Vegfa* expression in the limb mesenchyme drives the rearrangement of the vascular plexus into a highly patterned network. This includes a single axial artery that splits into a network of small capillaries, which drain into a thicker marginal vein (Eshkar-Oren et al., 2009).

In this study, we revisit the role of $S1P_1$ in angiogenesis based on our finding that at early stages of limb development the vasculature lacks mural cell coating. We show that $S1P_1$ acts independently of mural cells and EC-autonomously to inhibit sprouting angiogenesis, thereby promoting vessel stability. We then demonstrate in zebrafish the evolutionary conservation of this mechanism. Finally, we propose a model for sprouting angiogenesis whereby regulatory interaction between Vegfa and $S1P_1$ maintain balance between induction and restriction of this process.

MATERIALS AND METHODS

Mice

S1P$_1^{-/-lacZ}$ and *S1P$_1^{loxP/loxP}$* embryos were genotyped as previously described (Chae et al., 2004). To obtain endothelial-specific *S1P$_1$* knockout, *S1P$_1^{loxP/loxP}$* mice were crossed with mice expressing Cre recombinase under the control of the EC-specific promoter VE-Cadherin-Cre (Jackson Laboratories). The offspring was crossed with *S1P$_1^{loxP/loxP}$* to obtain *S1P$_1^{loxP/loxP}$VECad-Cre* embryos. The generation of *floxed-Vegfa* (Gerber et al., 1999), *floxed-Hif1a* (Ryan et al., 2000) and *Prx1* (also known as *Prrx1* – Mouse Genome Informatics)-*Cre* mice (Logan et al., 2002) have been described previously.

Inducible *Vegfa* overexpression in the limb mesenchyme was carried out by the reverse tetracycline transactivator (rtTA)/tetracycline-responsive element (tetO)-driven transgene system (Belteki et al., 2005; Gossen et al., 1995), with *Prx1-Cre* mouse (Logan et al., 2002) as an inducer. Briefly, *tetO-Vegfa* mice were crossed with *rtTA* mice. Mice heterozygous for *rtTA* and *tetO-Vegfa* (*rtTA-tetO-Vegfa*) were crossed with mice heterozygous for *Prx1-Cre* transgene as an inducer. To induce *Vegfa* expression, doxycycline was administered to pregnant females starting at embryonic day (E) 8.5 and embryos heterozygous for *Prx1-Cre*, *rtTA* and *tetO-Vegfa* (*Prx1-rtTA-tetO-Vegfa*) were compared with embryos heterozygous for *rtTA* and *Prx1-Cre* alleles (control).

In all timed pregnancies, plug date was defined as E0.5. For harvesting of embryos, timed-pregnant female mice were sacrificed by CO_2 intoxication. The gravid uterus was dissected out and suspended in a bath of cold PBS, and the embryos were harvested after amnionectomy and removal of the placenta. Tail genomic DNA was used for genotyping.

Zebrafish husbandry and morpholino oligonucleotide (MO) injection

Fish were bred and raised under standard conditions (Kimmel et al., 1995). *Tg(fli1:egfp)^{y1}* embryos were produced and staged as previously described (Yaniv et al., 2006). *s1p$_1$* antisense MOs (Gene Tools) were designed against the start codon/5′UTR to block translation (AGTGTCTGGCGATTAGGTCATCCAT). MOs were injected into *Tg(fli1:egfp)^{y1}* embryos at the one-cell stage and analyzed morphologically at 2-3 days post fertilization (dpf).

mRNA rescue experiment

The following primers were used to amplify the full-length coding sequences of zebrafish *s1p$_1$*: forward, 5′-ATGGAcGAtCTgATtGCtAGgCAtTACAACTTCACTGGGA-3′; reverse, 5′-TCTAGAACAGTCCCTTTAAG-3′. To prevent *s1p$_1$* MO binding to injected mRNA, the sequence of the MO binding site was modified such that it would not affect amino acid sequence (represented by lower case letters in the forward primer). After TOPO cloning and sequencing (Invitrogen, Carlsbad, CA, USA), a Gateway-compatible middle entry clone (Invitrogen) was generated using Gateway BP clonase (Invitrogen)-mediated recombination. The *s1p$_1$* coding sequences was then transferred into a pCSDest vector using Gateway LR clonase (Invitrogen)-mediated reaction to produce the pCS*s1p$_1$*CDS plasmid. After linearization with *Not*I, plasmids were used as templates for mRNA synthesis. Capped sense RNA was synthesized using SP6 RNA polymerase and the mMESSAGE mMACHINE system (Ambion, Austin, TX, USA). One-cell-stage embryos were microinjected with *s1p$_1$* mRNA and antisense MOs.

In situ hybridization

Zebrafish whole-mount in situ hybridization was performed as previously described (Thisse and Thisse, 2008). Antisense probes were generated using the following primers: *s1p$_1$*: forward, GCACCC-CTCTGTGGCCTGTG; reverse, GGCGGCGATGAACCAGACGG.

Inhibition of Flk1

SU5416 (Sigma) dissolved in DMSO was added to the culture media solution at a final concentration of 5 μM. Dechorionated zebrafish embryos [20 hours post fertilization (hpf)] were subjected to SU5416 treatment for 1 hour, then the chemical was washed and embryos were allowed to develop until 48 hpf.

Microscopy and imaging

Confocal imaging was performed using a Zeiss LSM 780 upright confocal microscope (Carl Zeiss, Jena, Germany) with a W-Plan Apochromat ×20 objective, NA 1.0. eGFP was excited with a 488 nm argon laser. Long-term, time-lapse in vivo imaging of zebrafish embryos was performed as previously described (Yaniv et al., 2006). *z*-stacks were acquired at 2.5-μm increments every 12 minutes. Images were processed off-line with ImageJ (NIH).

Quantitative RT-PCR (qRT-PCR)

For qRT-PCR analysis, 1 μg total RNA was used to produce first-strand cDNA. Reverse transcription was performed with SuperScriptII (Invitrogen) according to the manufacturer's protocol. qRT-PCR was performed using SYBR Green (Roche). Values were calculated using the second derivative method and normalized to *Gapdh* rRNA expression. For Vegfa, the primers used were: 5′-ACAGAAGGAGAGCAGAAGTC-CCAT-3′ (forward) and 5′-CACACAGGACGGCTTGAAGATGTA-3′ (reverse).

Whole-mount and section immunofluorescence

For whole-mount immunofluorescence, freshly dissected tissues were fixed overnight in 4% paraformaldehyde (PFA), transferred to PBS, then dehydrated to methanol and stored at –20°C until use. Samples were rehydrated to PBS and incubated for 2 hours in blocking solution (PBS containing 10% normal goat serum and 1% Triton X-100) and then incubated overnight at 4°C with primary antibody rat anti-PECAM (CD31; BD Pharmingen, San Diego, CA, USA) diluted 1:50 in blocking solution. Samples were washed in PBS containing 1% Triton X-100 at room temperature for 4 hours, and then incubated overnight at 4°C with biotinylated anti-rat secondary antibody (diluted 1:100; Vector Laboratories) and Cy2-conjugated streptavidin antibody (1:100; Jackson ImmunoResearch, West Grove, PA, USA) diluted in 1% BSA in PBS.

For section immunofluorescence, embryo limbs were embedded in OCT (Tissue-Tek) after 2-6 hours fixation in 4% PFA and 10 μm-thick cryostat sections were made. Cryosections were postfixed for 30 minutes in 4% PFA and permeabilized with 0.2% Triton in PBS. In order to block nonspecific binding of immunoglobulin, sections were incubated with 7% goat serum in PBS. Following blockage, cryosections were incubated

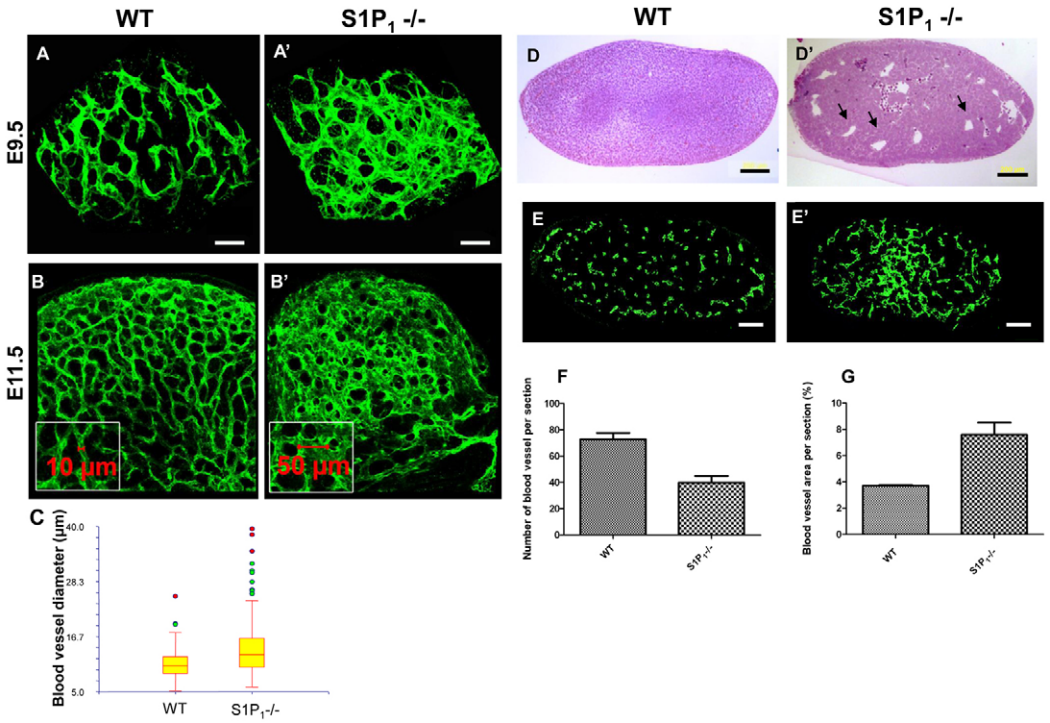

Fig. 1. Defective vasculature in *S1P$_1$*$^{-/-}$ mouse limb. (**A-B′**) Whole-mount forelimbs of E9.5 and E11.5 WT (A,B) and *S1P$_1$*$^{-/-}$ (A′,B′) mice were stained with anti-CD31 (green). (**C**) Vessel diameter measurements in E9.5 WT and *S1P$_1$*$^{-/-}$ forelimbs. Both limbs of four WT and four knockout (KO) embryos were analyzed; 35-40 vessels were measured in each limb, $P \leq 0.0001$. Boxes represent data from 25th to 75th percentile, horizontal lines represent median value and whiskers represent data from minimum to maximum excluding far out values, which are displayed as separate circles. (**D**,**D′**) Cross sections of WT (D) and KO (D′) forelimbs stained with H&E. Arrows indicate enlarged vessels with wide lumen. (**E**,**E′**) Transverse sections of E11.5 WT (E) and *S1P$_1$*$^{-/-}$ (E′) limbs stained with anti-CD31 antibody. (**F**,**G**) Quantification of vessel number (F) and relative area (G) in cross-sections of E11.5 forelimbs from WT and *S1P$_1$*$^{-/-}$ mice (n=8 sections from WT and 8 from S1P$_1$$^{-/-}$, P<0.001, error bars represent s.e.m.). Scale bars: in A,A′,B′, 50 µm; in B, 10 µm; in D,D′, 200 µm; in E,E′, 100 µm.

overnight at 4°C with primary antibodies: rat anti-CD31 (BD Pharmingen; diluted 1:100), rat anti-NG2 (Millipore; 1:200), rabbit anti-desmin (Dako Cytomation; 1:100) rabbit anti-β-galactosidase (Immunology Consultants Laboratory; 1:200). Sections were then washed in PBS and incubated with secondary fluorescent antibodies: Cy2 anti-rabbit (1:100; Jackson Laboratories) or Alexa Fluor 488-labeled goat anti-rat IgG (Molecular Probes). Samples were then washed and mounted on glass slides. For immunofluorescence staining of mural cells, samples were sectioned by vibrotome at 70 µm. Whole-mounts and sections were examined with an LSM 510 laser-scanning confocal microscope (Carl Zeiss).

Statistical methods

Variables are presented as mean ± s.e.m. In all measured variables but one, comparison between wild-type (WT) and mutant embryos was carried out using Student's *t*-test and statistical significance was defined as $P \leq 0.05$. Comparison of blood vessel diameter between WT and *S1P$_1$*$^{-/-}$ mouse embryos was carried out using the Mann-Whitney U test (also known as Wilcoxon rank-sum test).

RESULTS

Increased blood vessel diameter in limbs of *S1P$_1$*$^{-/-}$ mouse embryos

To elucidate the possible role of S1P$_1$ in vascular remodeling, we revisited the vascular phenotype in the developing limb of *S1P$_1$*$^{-/-}$ mice. To study the spatial organization of the limb vasculature, we performed whole-mount immunostaining of E9.5 and E11.5 wild-type (WT) and *S1P$_1$*$^{-/-}$ mouse forelimbs using an anti-CD31 antibody, which marks ECs. Whereas the vasculature in WT limbs comprised a uniform capillary network of small tubes that were distributed throughout the limb bud (Fig. 1A,B), the *S1P$_1$*$^{-/-}$ limb vasculature lacked organization and consisted of vessels with increased lumen diameter (Fig. 1A′,B′). The effect of *S1P$_1$* loss of function could be detected as early as E9.5, the onset of limb formation. At that stage, an increase of ~30% in vessel diameter was observed in *S1P$_1$*$^{-/-}$ forelimbs, relative to control limbs (Fig. 1C). At E11.5, the phenotype deteriorated and resulted in extremely enlarged vessels (Fig. 1B′). Hematoxylin and Eosin (H&E) staining of E11.5 limb cross-sections further validated the formation of enlarged vessels in the *S1P$_1$*$^{-/-}$ limbs (Fig. 1D,D′). Quantitative analysis of cross-sections from WT and *S1P$_1$*$^{-/-}$ limbs (Fig. 1E,E′) showed a significant reduction in vessel number and a significant increment in total vessel density in *S1P$_1$*$^{-/-}$ embryos (Fig. 1F,G).

Together, these results suggest that S1P$_1$ plays a central role in limb vascular remodeling.

S1P$_1$ regulates vascular remodeling independently of mural cells

As mentioned, S1P$_1$ has been implicated in vascular stabilization by mediating the interaction between ECs and mural cells (Allende et al., 2003; Liu et al., 2000; Paik et al., 2004). As mural cells were previously suggested to promote vascular stability (Benjamin et al., 1998; von Tell et al., 2006), this mediating role of S1P$_1$ could explain the defects in vascular remodeling observed in its absence. In order to explore this hypothesis, we examined the maturation

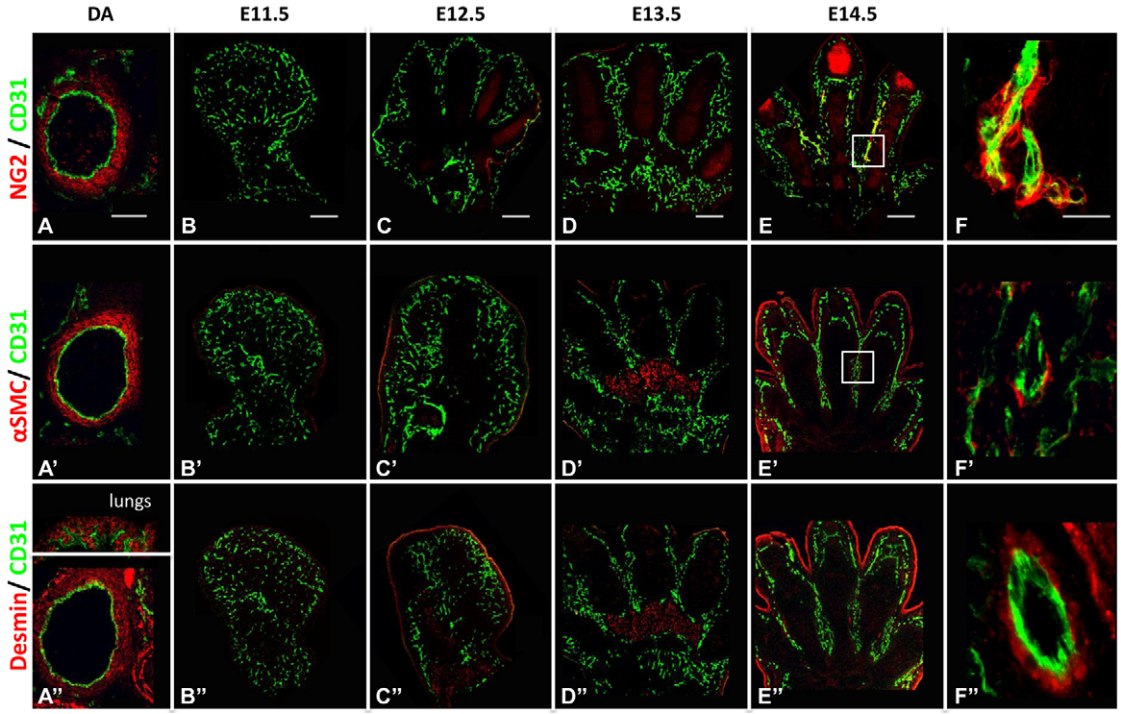

Fig. 2. Blood vessels lack mural cells at early stages of limb development. (**A-F″**) Dorsal aorta sections (A-A″) and forelimbs of E11.5-14.5 control mouse embryos (B-F″) immunostained with antibodies against NG2, α-smooth muscle actin (αSMC) and desmin to detect smooth muscle cells and pericytes (red) and with anti-CD31 antibody for ECs (green). F and F′ show magnifications of the boxed areas in E and E′, respectively. F″ shows magnification of a proximal blood vessel from the limb shown in E″. Scale bars: in A-A″, 100 μm; in B-E″, 200 μm; in F-F″, 20 μm.

state of limb vessels by immunostaining sections from E11.5-14.5 WT mouse embryos with three different markers for smooth muscle cells and pericytes, namely NG2 (Cspg4 – Mouse Genome Informatics), α-smooth muscle actin and desmin (Fig. 2). Examination showed that mural cells were absent from the vasculature at E11.5 (Fig. 2B-B″) and were observed only between E13.5 and E14.5 (Fig. 2E-F″).

Our finding that during the initial stages of limb development the vasculature consists of an EC network that has not undergone maturation, combined with the vascular aberrations observed in $S1P_1^{-/-}$ limbs as early as E9.5, strongly suggest a new, mural cell-independent role for $S1P_1$ in vascular remodeling.

$S1P_1$ regulates vascular remodeling EC-autonomously

Our finding that $S1P_1$ is necessary for vascular remodeling independently of mural cells raised the question of whether its activity is autonomously required by ECs. To address this question, we first analyzed *S1P1*-expressing cells in E11.5 limbs by using mice with a *lacZ* cassette in the *S1P1* locus (Liu et al., 2000). Cross sections of $S1P_1^{+/-lacZ}$ forelimbs were immunostained with antibodies for β-galactosidase and CD31, as markers for $S1P_1$ and ECs, respectively. As seen in Fig. 3A-C, *S1P1* expression was restricted to ECs in the developing limb. We next deleted *S1P1* specifically in ECs by using the VE-cadherin-*Cre* mouse ($S1P_1^{loxP/loxP}$-*VECad-Cre*). Cross and longitudinal sections of E13.5 control and conditional knockout (cKO) forelimbs were stained with H&E (Fig. 3D-G′) or immunostained with anti-CD31 (Fig. 3H-L′). Notably, EC-specific *S1P1* cKO mice exhibited similar vascular phenotypes to those observed in limbs of *S1P1*-null embryos, namely vessels with increased lumen diameter. Together, these results imply that $S1P_1$ regulates vascular remodeling in an EC-autonomous manner.

Regulatory role of $S1P_1$ in vascular remodeling is evolutionarily conserved

Our finding of a new, mural cell-independent role for $S1P_1$ in vascular development prompted us to study its involvement in this process in zebrafish embryos, in which the vasculature consists of an EC network until 72 hpf (Santoro et al., 2009). Because the expression profile of *s1p1* (*s1pr1* – Zebrafish Information Network) has not been previously characterized in zebrafish, we first performed in situ hybridization (ISH) for *s1p1* in developing embryos. As can be seen in Fig. 4, ISH results demonstrated a dynamic expression pattern during 24-52 hpf, which was similar to the pattern observed in mouse embryos (Liu et al., 2000; Meng and Lee, 2009). Notably, *s1p1* expression was prominent in the zebrafish neural tube and vasculature.

Next, to study the role of $S1p_1$ in vascular development, we knocked down $S1p_1$ by translational blocking antisense morpholino (*s1p1* MO) in *Tg(fli:egfp)*^{y1} embryos (Isogai et al., 2003). The morphant embryos showed several developmental defects at 3 dpf. These included hindbrain malformations, pericardial edema and heart defects (Fig. 5A,B). These malformations were similar to the defects observed in $S1P_1^{-/-}$ mice (Allende and Proia, 2002). To demonstrate the specificity of the knockdown effect, we rescued the phenotype by injection of *s1p1* RNA to *s1p1* MO embryos (supplementary material Fig. S1).

Examination of the vasculature of *s1p1* MO embryos revealed several vascular defects. In zebrafish, the onset of intersegmental vessel (ISV) formation is at 24 hpf, as ECs from the dorsal aorta

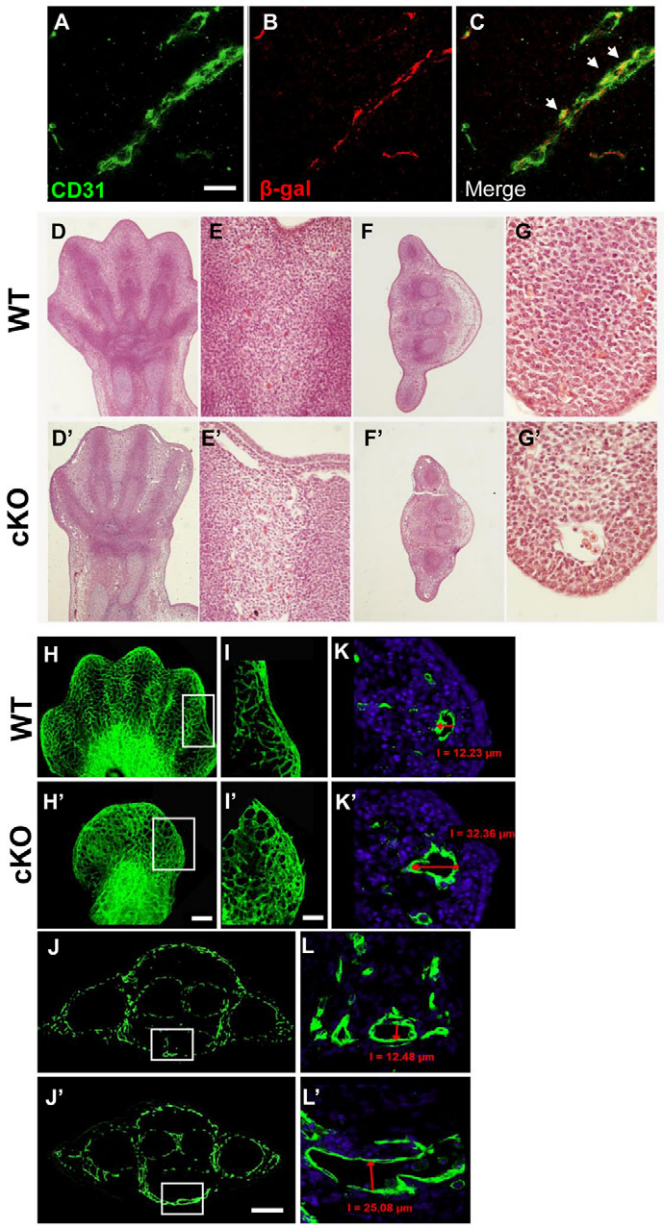

Fig. 3. EC-autonomous role for S1P$_1$ in limb vascular development. (**A-C**) Forelimbs of E11.5 *S1P$_1$*$^{+/-lacZ}$ mouse embryos stained for ECs with anti-CD31 (A) and β-galactosidase (B); arrows indicate *S1P$_1$*-expressing ECs (C). (**D-L'**) Defective vasculature in EC-specific *S1P$_1$* cKO embryos at E13.5. Transverse and longitudinal sections of control (D-G) and *S1P$_1$*$^{loxP/loxP}$*VECad-Cre* (D′-G′) littermate limbs at E13.5 were stained with H&E. Whole-mounts and cross-sections of forelimbs from E13.5 WT (H-L) and *S1P$_1$* cKO (H′-L′) mice were immunostained with anti-CD31 (green). I and I′ show magnifications of the boxed areas in H and H′, respectively. K and K′ show magnifications of the marginal vein and measurement of its diameter (marked by red arrows). L and L′ show magnifications of the boxed areas in J and J′, respectively; red arrows indicate diameter measurements. Scale bars: in A-C, 20 µm; in H,H′, 200 µm; in I,I′, 100 µm; in J,J′, 200 µm.

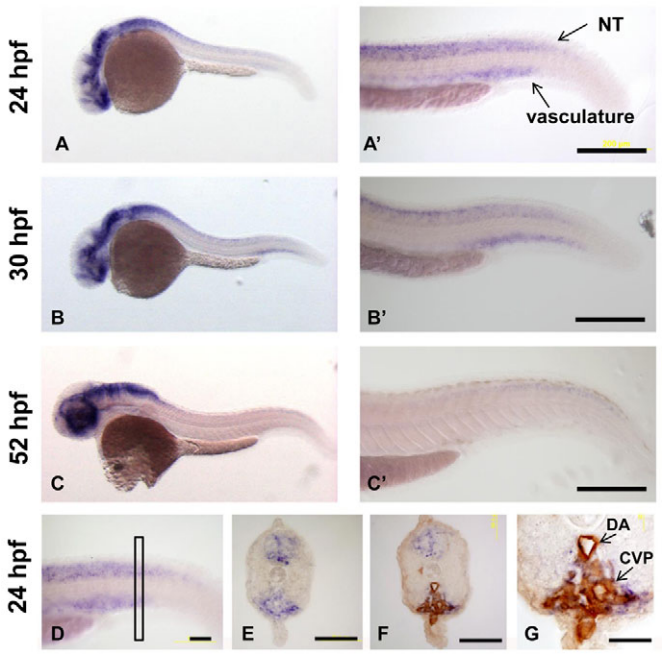

Fig. 4. Expression profile of *s1p$_1$* during zebrafish embryonic development. (**A-G**) In situ hybridization for *s1p$_1$* in zebrafish embryos at 24 hpf (A,A′), 30 hpf (B,B′) and 52 hpf (C,C′). A′, B′ and C′ show magnifications of the tail area shown in A, B and C, respectively. NT, neural tube. (D) Lateral view of the tail at 24 hpf. (E) Cross-section from the rectangular area marked in D. (F) Cross-section of *Tg(fli-egfp)*^{y1} zebrafish embryo counter-immunostained with anti-GFP antibody to mark blood vessels. (G) Magnification of F; both the dorsal aorta (DA) and the caudal vein plexus (CVP) show *s1p$_1$* expression. Scale bars: in A-C′, 200 µm; in D-F, 50 µm; in G, 20 µm.

(DA) begin to migrate dorsally. In *s1p$_1$* MO embryos, a delay in EC migration was observed (Fig. 5C). Quantitative analysis revealed shorter ISVs, compared with the WT (Fig. 5D). In addition, whereas in the WT most of the ISVs reached the midline, in *s1p$_1$* MO embryos these vessels remained below the midline (Fig. 5E). Eventually, the migration and formation of these vessels was accomplished (supplementary material Fig. S2).

These results further support the notion that S1P$_1$ regulates vascular remodeling by affecting EC behavior prior to maturation.

S1P$_1$ negatively regulates sprouting angiogenesis

The abnormal vessel size observed in mice could be the consequence of excessive sprouting. To study the possible role of S1p$_1$ in sprouting angiogenesis, we used the mutant zebrafish model. We focused on the ISVs and on the caudal vein plexus (CVP) (Fig. 6A), which form by this process in zebrafish (Choi et al., 2011; Zhong, 2005). In control embryos, the ISV sprouted from the dorsal aorta at 24 hpf by extending numerous long filopodia (Fig. 6B). These sprouts stretched between each pair of somites and anastomosed to give rise to the dorsal longitudinal anastomotic vessel (DLAV). At 48 hpf, when ISV formation was completed, the filopodia that had been instrumental for this process stopped forming. Examination of the ISV sprouting process in *s1p$_1$* MO embryos (Fig. 6B) revealed comparable filopodial numbers with control embryos at 24 hpf (Fig. 6B′). However, at 48 hpf, the morphant's ISV continued to extend numerous filopodia in all directions.

Unlike the ISV, the CVP forms as a very dense capillary network (Choi et al., 2011; Wiley et al., 2011). To maintain this structure and prevent fusion of forming vessels, inhibition of excessive filopodia formation is crucial. Analysis of the axial

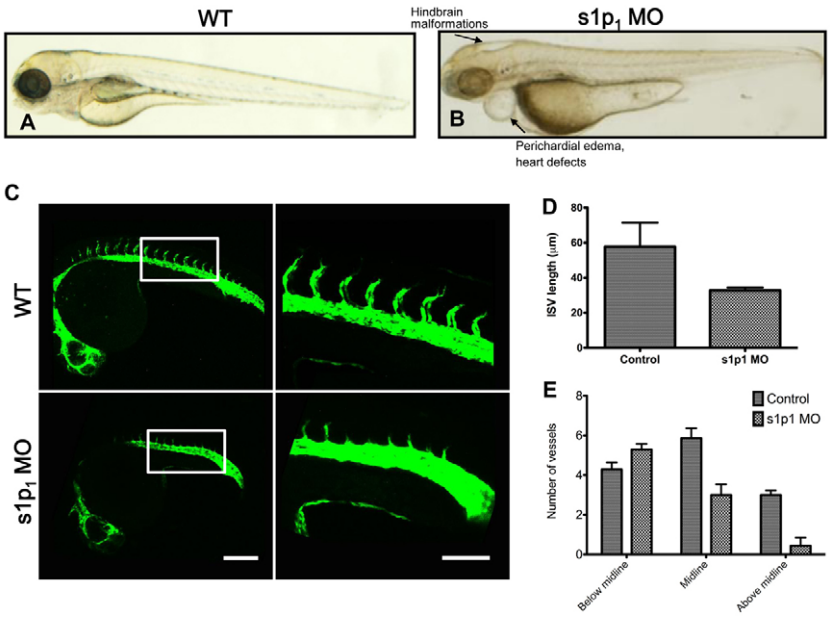

Fig. 5. *s1p1* knockdown in zebrafish causes defects in blood vessel formation. *Tg(fli-egfp)*^{y1} zebrafish embryos were injected with a control MO and a translation-blocking *s1p1* MO and analyzed at 3 dpf. (**A**,**B**) Bright-field images of control and *s1p1* MO embryos. Arrows in B indicate hindbrain malformations, pericardial edema and heart defects observed in the mutant. (**C**) Fluorescence microscopy of control and *s1p1* MO embryos at 24 hpf. Right-hand panel shows magnifications of the boxed areas on the left. (**D**) Measurements of ISV length (corresponding to the boxed area in C) in control and *s1p1* MO embryos (n=8 WT and 8 MO embryos, P<0.0001, error bars represent s.e.m.). (**E**) Quantification of ISV location relative to the midline (n=10 WT and 10 MO embryos; 6-8 ISVs from each embryo were analyzed, P<0.05, error bars represent s.e.m.). Scale bars: in C, left panel, 200 μm; in C, right panel, 100 μm.

vessel at the caudal part of the *s1p1* MO embryo at 48 hpf showed failure of the CVP to remodel into a capillary network (Fig. 6C). The CVP appeared to be fused in *s1p1* MO embryos, whereas WT siblings displayed a clear network with spaces between capillaries (Fig. 6C′).

In order to analyze these differences in more detail, we followed the formation of the CVP in vivo by long term, time-lapse imaging. WT embryos exhibited ECs that extended filopodia, which eventually met and formed capillary loops. Once these loops formed, the number of filopodia decreased, preventing the capillaries from further fusion and thereby preserving their structure and size (Fig. 7A; supplementary material Movie 1). In contrast to this tightly regulated process, ECs in *s1p1* MO embryos continued to sprout and to extend numerous filopodia even when capillary loops were fully established. This resulted in the formation of supernumerary connections between adjacent sprouts, with a concomitant reduction in the space between capillary loops. Ultimately, the hypersprouting capillaries fused to form one thick vessel instead of a well-defined plexus (Fig. 7A; supplementary material Movie 2).

Next, we analyzed EC sprouting in mouse forelimbs at E9.5. WT limbs exhibited low numbers of filopodial extensions (Fig. 7Ba,Bb). By comparison, the *S1P1*$^{-/-}$ limb vasculature exhibited an increase in EC filopodia (Fig. 7Bc,Bd). In addition, whereas most of the filopodia in the WT made no connection with adjacent vessels, the filopodia in the *S1P1*$^{-/-}$ limb extended from one vessel to another, establishing ectopic interconnections (Fig. 7Bd). Those interconnections might have caused fusion of adjacent capillaries, which would explain the reduction in vessel number observed at E11.5 (Fig. 1F).

Together, these results suggest a crucial role for $S1P_1$ in the termination of sprouting angiogenesis during vascular remodeling.

$S1P_1$ inhibits both Vegfa-dependent and -independent sprouting angiogenesis

Vegfa is a key regulator of sprouting angiogenesis that was previously shown to control vascular development in the limb (Eshkar-Oren et al., 2009). One way by which $S1P_1$ can inhibit sprouting is by negatively regulating Vegfa activity. This would imply that elevation of Vegfa signaling should lead to a similar vascular phenotype as observed in the *S1P1*$^{-/-}$ limb. To overexpress *Vegfa* specifically in the forming limb, we used a triple transgenic mouse system, in which the expression of the reverse tetracycline

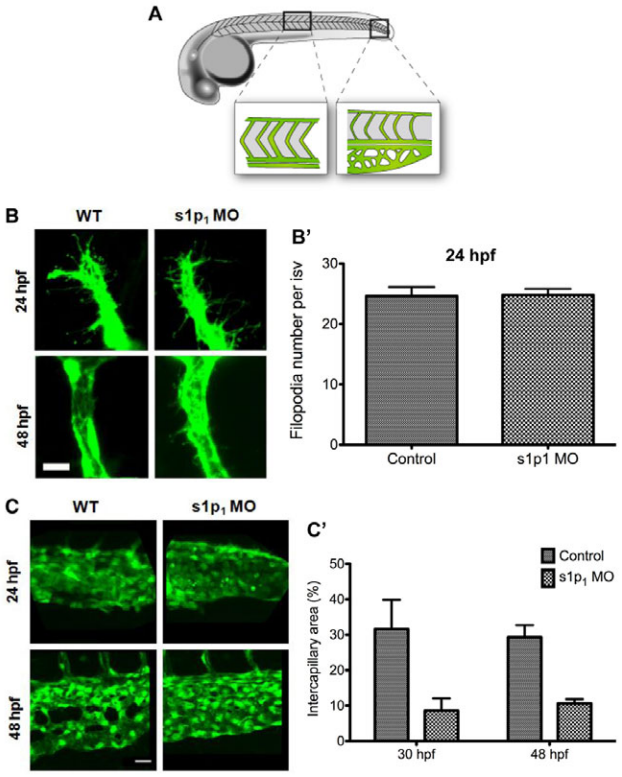

Fig. 6. *s1p1* MO embryos exhibit remodeling defects in the ISV and CVP. (**A**) Schematic showing the anatomical location of the areas shown in B and C. (**B**,**C**) Fluorescence microscopy of the ISV (B) and CVP (C) regions in WT and *s1p1* MO *Tg(fli-egfp)*^{y1} zebrafish embryos at 24 and 48 hpf. (**B′**) Graph showing comparable filopodia numbers in ISV of WT and *s1p1* MO zebrafish (n_{wt}=11, n_{s1p1MO}=16, P=0.92). (**C′**) Graph showing comparison of the intercapillary area in the CVP between WT and *s1p1* MO zebrafish (n_{wt}=7, $n_{s1p1\ MO}$=7, P=0.002, error bars represent s.e.m.). Scale bars: in B, 10 μm; in C, 20 μm.

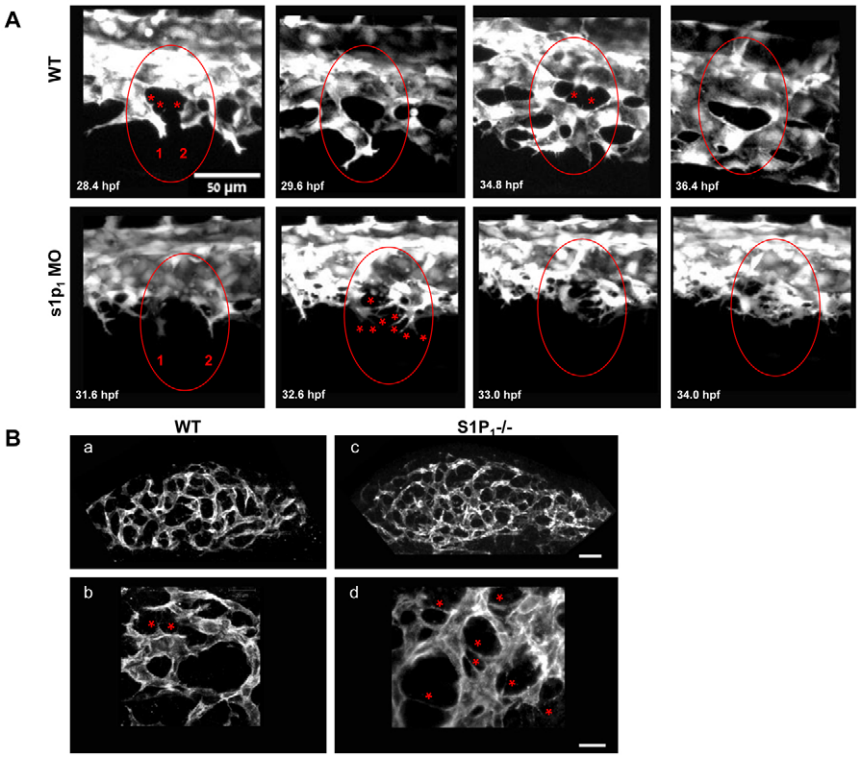

Fig. 7. Excessive filopodia formation leads to aberrant vascular remodeling in *s1p$_1$* MO zebrafish and *S1P$_1^{-/-}$* mouse embryos. (**A**) Sequential confocal microscopy images showing lateral views of the CVPs from WT and *s1p$_1$* MO *Tg(fli-egfp)^{y1}* zebrafish embryos. Circles demarcate two sprouts, marked as 1 and 2, in WT and *s1p$_1$* MO embryos that extend filopodia (marked with asterisks). This results in the formation of a capillary loop in the WT and in over-sprouting and fusion in the mutant. For visualization of the entire sequence, see supplementary material Movies 1 and 2. (**B**) Immunofluorescent staining with anti-CD31 of whole-mount forelimbs from E9.5 WT (a,b) and *S1P$_1^{-/-}$* (c,d) mice; b and d show magnifications of a and c, respectively. Asterisks indicate excessive filopodia in *S1P$_1^{-/-}$* limbs, compared with WT limbs. Scale bars: in a,c, 50 μm; in b,d, 20 μm.

transactivator (*rtTA*) and the tetracycline-responsive element (*tetO-Vegfa*) was induced by *Prx1-Cre* (Belteki et al., 2005; Gossen et al., 1995). As can be seen in Fig. 8A,B, the vasculature in *Vegfa*-overexpressing limbs consisted of vessels with increased lumen diameter relative to the WT, as was observed for *S1P$_1^{-/-}$* limbs.

Previous studies also reported increased *Vegfa* expression in E11.5 *S1P$_1^{-/-}$* limbs (Chae et al., 2004). To address the possibility that the vascular phenotype in *S1P$_1^{-/-}$* limbs was a result of elevated *Vegfa* expression, we compared the progression of the vascular phenotype with the expression profile of *Vegfa*. As mentioned, abnormal vasculature was evident in *S1P$_1^{-/-}$* limbs as early as E9.5, at the onset of limb formation (Fig. 1A-B′, Fig. 7B). However, quantification of *Vegfa* expression by qRT-PCR at that stage revealed comparable levels in *S1P$_1^{-/-}$* and WT limbs (Fig. 8C). This suggests that initially, vascular defects in *S1P$_1^{-/-}$* mutant are not a result of an increase in *Vegfa* levels. Yet, at a later stage (E11.5), *Vegfa* was upregulated in *S1P$_1^{-/-}$* limbs relative to the control (Fig. 8D), suggesting that *Vegfa* might contribute to the progression and severity of the phenotype.

Although we ruled out the possibility that *Vegfa* upregulation was the mechanism underlying hypersprouting in *S1P$_1^{-/-}$* limbs, S1P$_1$ could still regulate sprouting angiogenesis by antagonizing Vegfa activity. To test this supposition, we either blocked or attenuated *Vegfa* expression in limbs of *S1P$_1^{-/-}$* embryos and examined the effect on the vascular phenotype. To block *Vegfa* expression in limb mesenchyme of *S1P$_1^{-/-}$* embryos, we used *Prx1-Cre* as a deleter (*Vegfa$^{loxP/loxP}$Prx1-Cre, S1P$_1^{-/-}$*) (Logan et al., 2002). To reduce its levels, we deleted the expression of *Hif1a* (*Hif1a$^{loxP/loxP}$Prx1-Cre*), a well-documented transcriptional regulator of *Vegfa* (Forsythe et al., 1996; Liu et al., 1995). Previously, we showed that conditional knockout of *Hif1a* in mouse limb mesenchyme, using *Prx1-Cre*, results in a 30% reduction in *Vegfa* expression (Amarilio et al., 2007). Whole-mount forelimbs from WT, *S1P$_1^{-/-}$*, *S1P$_1$-Vegfa* double knockout (dKO) and *S1P$_1$-Hif1a* dKO embryos at E11.5 were stained with CD31 (Fig. 8E-R). As shown before, *S1P$_1^{-/-}$* forelimbs exhibited severe defects in limb vasculature that included enlarged vessels and an increase in vessel sprouting (Fig. 8G,H). In contrast to the *S1P$_1^{-/-}$* phenotype, *Vegfa* KO in limb mesenchyme led to a dramatic decrease in blood vessel density in the forelimb (Fig. 8I,J). Interestingly, the phenotype of the dKO mice was similar to the phenotype of the *Vegfa* KO mice, with no trace of the hypersprouting observed in the *S1P$_1^{-/-}$* mice (Fig. 6K,L). Limbs of *S1P$_1$-Hif1a* dKO embryos exhibited a partial rescue of the *S1P$_1^{-/-}$* phenotype, as there was a reduction in vessel density and diameter and only a few large vessels (Fig. 6Q,R).

Together, these results strongly imply that the effect of S1P$_1$ on vascular development is *Vegfa*-dependent, suggesting that S1P$_1$ negatively regulates induction of sprouting angiogenesis by Vegfa.

These findings in mice prompted us to investigate whether this genetic interaction between *s1p$_1$* and *vegfa* is conserved in zebrafish. In a previous study, *vegfa* overexpression in zebrafish resulted in two subintestinal vessel (SIV) phenotypes, namely dilated vessels and ectopic sprouting (Serbedzija et al., 1999). These phenotypes are similar to those observed in *s1p$_1$* MO embryos (supplementary material Fig. S2). To examine the interaction between *s1p$_1$* and *vegfa*, SU5416, an inhibitor of the Vegfa receptor Flk1 (Kdrl – Zebrafish Information Network), was administered to *s1p$_1$* MO and WT embryos. As shown previously (Serbedzija et al., 1999), blockade of the Vegfa pathway using SU5416 inhibits SIV development. As expected, *s1p$_1$* MO embryos treated with SU5416 showed a similar phenotype (Fig. 9), demonstrating the dependence of S1p$_1$ activity on Vegfa.

Interestingly, a recent study showed that CVP development is independent of *vegfa* (Wiley et al., 2011). This finding allowed to explore the possibility that S1p$_1$ can act independently of Vegfa. Indeed, blocking the Vegfa pathway using SU5416 in WT embryos had no effect on CVP development (Fig. 9); conversely, the

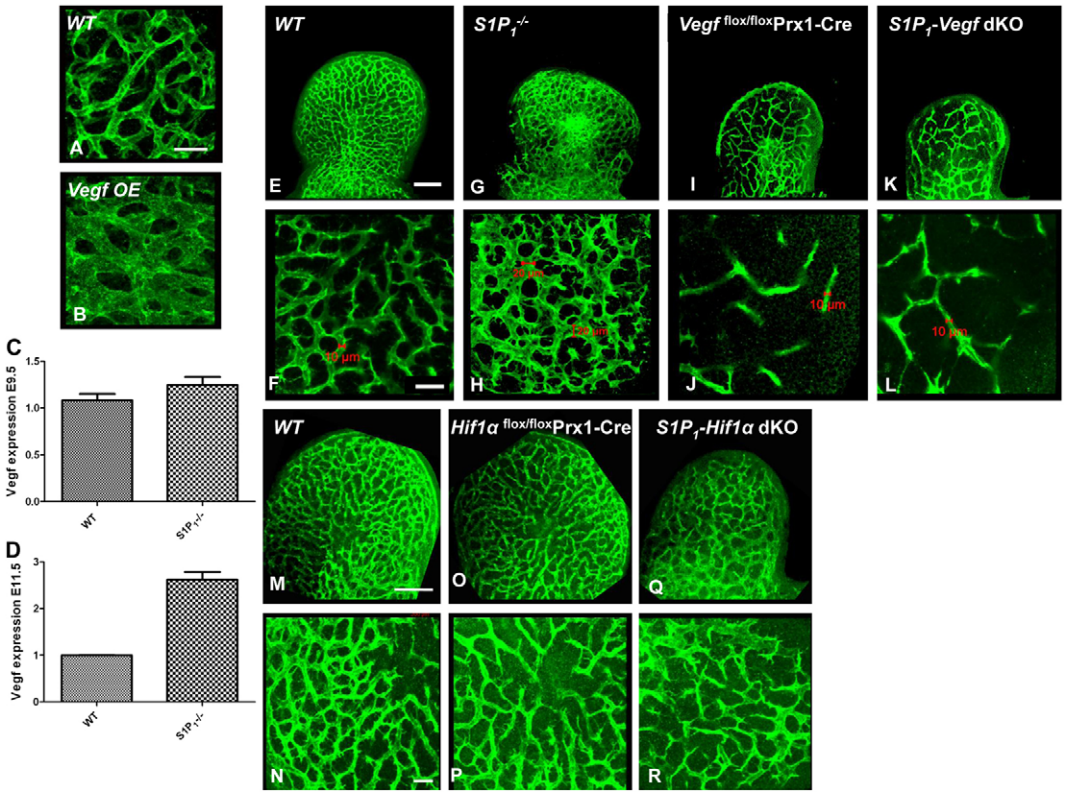

Fig. 8. The effect of S1P$_1$ on vascular development in mice is Vegfa dependent. (**A**,**B**) Immunofluorescent staining of whole-mount forelimbs of E10.5 WT (A) and *Vegfa* over-expressing (OE; B) mice. (**C**,**D**) *Vegfa* expression in WT and *S1P$_1$*$^{-/-}$ embryos assessed by qRT-PCR at E9.5 (C; *n*=4, *P*=0.2, not significant) and at E11.5 (D; *n*=5, *P*<0.0001). Data was normalized to *Gapdh*; error bars represent s.e.m. (**E-R**) Immunofluorescence staining of whole-mount forelimbs of E11.5 WT (E,F,M,N), *S1P$_1$*$^{-/-}$ (G,H), *Vegfa*$^{loxP/loxP}$*Prx1-Cre* (I,J), *Vegfa-S1P$_1$* dKO (K,L), *Hif1a*$^{loxP/loxP}$*Prx1-Cre* (O,P) and *Hif1a-S1P$_1$* dKO (Q,R) mice stained with CD31 (green). F, H, J, L, N, P, and R are 40× magnifications of the images in the respective panels above. Scale bars: in E,G,I,K,M,O,Q, 200 µm; in A,B,F,H,J,L,N,P,R, 50 µm.

SU5416 inhibitor did not rescue the CVP phenotype in *s1p$_1$* MO embryos. These intriguing results led us to conclude that in the CVP, S1p$_1$ regulates sprouting angiogenesis independently of Vegfa.

DISCUSSION

During organogenesis, the vasculature accommodates growing demands for oxygen and nutrients by remodeling into a complex network composed of different-sized vessels (Coffin and Poole, 1988; Drake et al., 1998; Flamme et al., 1995; Folkman, 2003; Risau and Flamme, 1995). Sprouting angiogenesis plays a central role in the remodeling process by forming new vascular loops, which expand the vascular network. Over the years, several signaling pathways have been identified to induce angiogenic sprouting (Adams and Alitalo, 2007; Eilken and Adams, 2010; Jakobsson et al., 2010). By contrast, we know little about the equally important mechanism that terminates this process to allow vascular stability. Our finding that S1P$_1$ negatively regulates the sprouting process, in both mouse and zebrafish embryos, provides an important molecular component in this mechanism. This finding provides an explanation for the cessation of filopodia extension once two tip cells have anastomosed and formed a new vascular loop. This is necessary to prevent excessive connections between tip cells, which would ultimately disrupt the organization of the vascular system. By restricting the sprouting process, S1P$_1$ acts as a control mechanism that stabilizes the newly formed network and prevents further sprouting.

Another mechanism that may promote vascular stabilization by restricting sprouting is the maturation process (Benjamin et al., 1998; von Tell et al., 2006). Previous studies have attributed the effect of S1P$_1$ on vascular development to its role in regulating interactions between ECs and mural cells during maturation (Allende and Proia, 2002; Liu et al., 2000). However, this mechanism cannot operate at developmental stages when vessels lack mural cell coverage. Our analysis shows that the limb bud vasculature is not invested by mural cells for several days of development. Delay in vascular maturation was also reported in the developing wing of chick embryos, in which the vasculature was not coated by VSMCs (Vargesson and Laufer, 2001). Our finding of abnormal vasculature prior to maturation in limbs in which *S1P$_1$* expression was blocked in ECs strongly suggests that S1P$_1$ has a previously undescribed, mural cell-independent role in vascular development.

Previous studies identify S1P as a pro-angiogenic factor (Schmid et al., 2007; Yonesu et al., 2009). By contrast, we show that S1P$_1$ acts to block sprouting and restrict angiogenesis. There can be several explanations for this difference. The most likely is that the pro-angiogenic effect was demonstrated in vitro, whereas our work was carried out in vivo. With regard to the mode of action by which S1P$_1$ negatively regulates sprouting, our study provides several pieces of evidence in support of the hypothesis that S1P$_1$

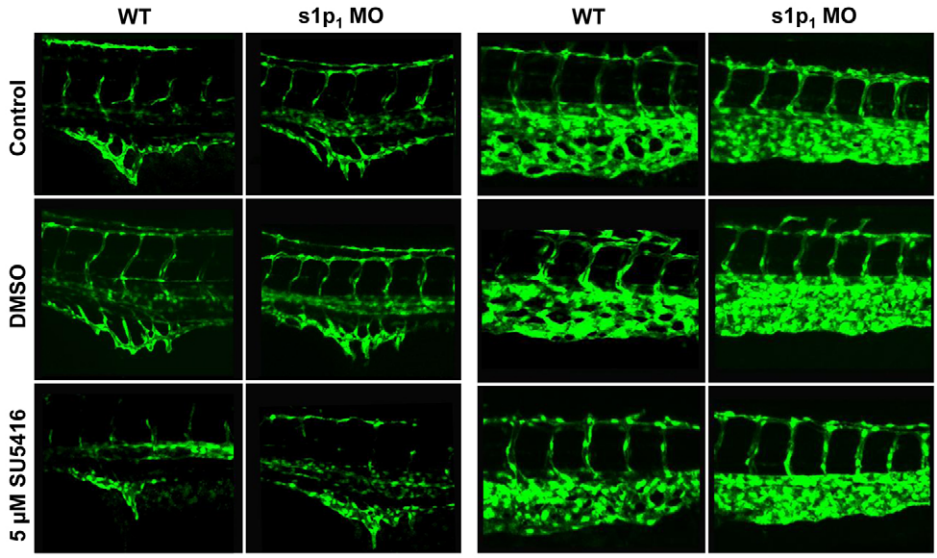

Fig. 9. Both Vegfa-dependent and -independent effects of S1p$_1$ on vascular development in zebrafish. Fluorescence microscopy of 48 hpf control and *s1p$_1$* MO zebrafish embryos**.** Left panel: SIV of untreated (control), DMSO-treated and 5 μM SU5416-treated embryos; right panel: CVP of untreated (control), DMSO-treated and 5 μM-SU5416 treated embryos.

restricts this process by antagonizing the activity of an angiogenic factor such as Vegfa. We show that increased expression of *Vegfa* in the limb led to vascular abnormalities similar to those observed upon *S1P$_1$* loss of function, whereas reduction in *Vegfa* expression rescued the S1P$_1$ phenotype. That *Vegfa* levels were initially comparable between WT and *S1P$_1^{-/-}$* mouse embryos negates the possibility that S1P$_1$ regulates *Vegfa* expression, leaving the point of interaction between these two pathways an open question. Nevertheless, S1P$_1$ signaling may also be involved in vascular remodeling independently of Vegfa signaling. Our finding that in *s1p$_1$* MO zebrafish embryos CVP development, which is not dependent on *vegfa* (Wiley et al., 2011), was affected clearly supports this possibility. Such a Vegfa-independent mechanism might involve regulation of cytoskeletal rearrangement and filopodia formation. Previous studies demonstrate the involvement of S1P$_1$ in the assembly of cortical actin by inducing redistribution of molecules such as cortactin and Arp2/3 (Lee et al., 2006). Disruption of this distribution might cause aberrant organization of actin in the cytoskeleton and disproportional filopodia formation. Further analysis is required to fully decipher the inhibitory effect of S1P$_1$ on angiogenic sprouting.

Another interesting question regards the mechanism that allows the formation of vessels with different sizes. Indications for such a mechanism are the two main phenotypes we observed both in mice and in zebrafish upon *S1P$_1$* loss of function, namely hypersprouting and increased vessel diameter. We show at early developmental stages (E9.5 in mice and 24 hpf in zebrafish) that the *S1P$_1$* loss-of-function phenotype commences with hypersprouting. As development proceeds, excessive sprouting induces fusion of sprouts that form one overly thick vessel instead of a well-defined plexus. The outcome of this process is reduced vessel number combined with increased vessel diameter. In light of this finding, it is tempting to speculate that sprouting may also serve as a mechanism that controls vessel diameter. This mechanism operates by maintaining the activity of tip cells after a loop has formed, leading eventually to the merging of newly formed loops into one larger vessel. Such a model was previously suggested by Drake and Little (Drake and Little, 1999).

In mice, *S1P$_1$* is expressed in endothelial cells and S1P is found in the blood serum (Hla et al., 2008; Yatomi et al., 2000). Given that S1P is secreted into the blood, a physiological feedback loop mechanism could explain the involvement of S1P$_1$ in sprouting angiogenesis (Fig. 10). Prior to the formation of a capillary loop, tip cells are poorly exposed to the blood stream and, as a

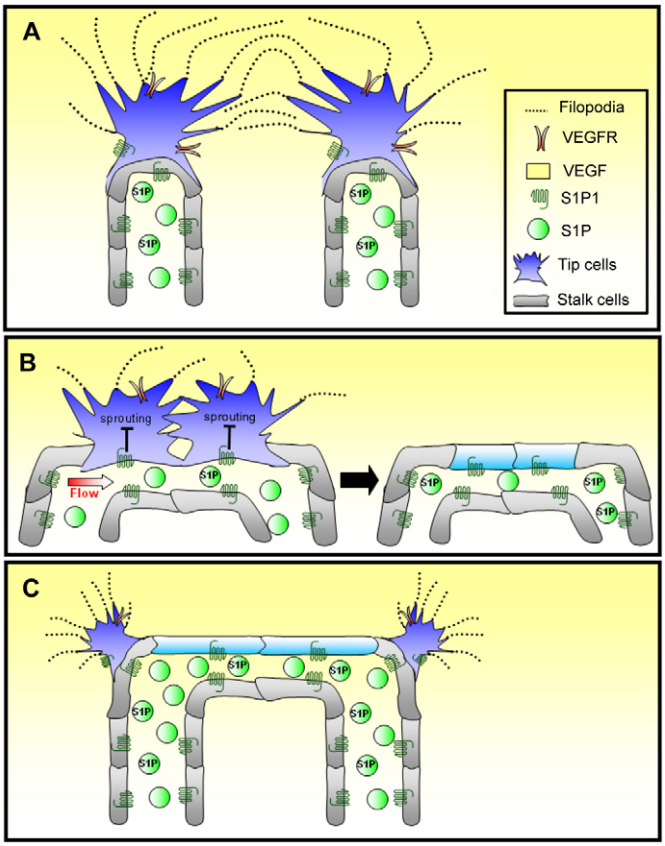

Fig. 10. The involvement of S1P$_1$ in vascular remodeling. A model illustrating the regulatory role of S1P$_1$, which acts to fine-tune angiogenesis during vascular remodeling. (**A**) Capillary loop formation: Vegfa induces formation of sprouts, which consist of tip and stalk cells. *S1P$_1$* is expressed by tip cell, which are poorly exposed to its ligand S1P in the blood stream. (**B**) Tip cells anastomose to form lumen and blood flow commences. (**C**) Once proper circulation is established, blood-borne S1P binds to S1P$_1$ and inhibits sprouting. Dotted lines represent filopodia.

consequence, to S1P. Once a functional capillary loop is formed, these cells come into contact with the blood stream that carries S1P. This enables S1P to interact with its receptor to inhibit the Vegfa pathway and thereby to terminate the sprouting process. In zebrafish, blood circulation starts at ~25 hpf, which coincides with the emergence of the vascular phenotype in the morphant. This concurrence supports the notion of a physiological feedback loop.

This study identifies $S1P_1$ as a major component in a mechanism that negatively regulates angiogenic sprouting. This mechanism acts EC-autonomously and independently of mural cell. Our findings provide a new module in the regulation of embryonic angiogenesis, which terminates sprouting to prevent excessive loop formation and stabilize the vascular network.

Acknowledgements
We are grateful to Dr Richard L. Proia for the $S1P_1$ and floxed-$S1P_1$ mice and to Dr C. Tabin for the *Prx1-Cre* mice. We thank Mr N. Konstantin for expert editorial assistance, and members of the Zelzer laboratory for advice and suggestions. We thank Vera Shinder from the Irving and Cherna Moskowitz Center for Nano and Bio-Nano Imaging at the Weizmann Institute of Science for her expertise in electron microscopy analysis; Prof. E. Schechtman for statistical consultation; and A. Mishali from the Graphic Design Department of Weizmann Institute of Science for help with the graphic model.

Funding
This work was supported by the Israel Science Foundation [grant 1206/09]; the Y. Leon Benoziyo Institute for Molecular Medicine; Helen and Martin Kimmel Institute for Stem Cell Research; J & R Center for Scientific Research; Yeda-Sela Center for Basic Research; Estate of Raymond Lapon; Estate of David Levinson; the Israel Science Foundation (ISF) Legacy Heritage Fund Morasha Biomedical program; Marla L. Schaefer (New York, NY, USA); The Leo and Julia Forchheimer Center for Molecular Genetics; The Stanley Chais New Scientist Fund; The Kirk Center for Childhood Cancer and Immunological Disorders; and The David and Fela Shapell Family Center for Genetic Disorders Research. E.Z. is the incumbent of the Martha S. Sagon Career Development Chair.

Competing interests statement
The authors declare no competing financial interests.

Supplementary material
Supplementary material available online at
http://dev.biologists.org/lookup/suppl/doi:10.1242/dev.078550/-/DC1

References

Adams, R. H. and Alitalo, K. (2007). Molecular regulation of angiogenesis and lymphangiogenesis. *Nat. Rev. Mol. Cell Biol.* **8**, 464-478.
Adams, R. H. and Eichmann, A. (2010). Axon guidance molecules in vascular patterning. *Cold. Spring Harb. Perspect. Biol.* **2**, a001875.
Allende, M. L. and Proia, R. L. (2002). Sphingosine-1-phosphate receptors and the development of the vascular system. *Biochim. Biophys. Acta* **1582**, 222-227.
Allende, M. L., Yamashita, T. and Proia, R. L. (2003). G-protein-coupled receptor S1P1 acts within endothelial cells to regulate vascular maturation. *Blood* **102**, 3665-3667.
Amarilio, R., Viukov, S. V., Sharir, A., Eshkar-Oren, I., Johnson, R. S. and Zelzer, E. (2007). HIF1alpha regulation of Sox9 is necessary to maintain differentiation of hypoxic prechondrogenic cells during early skeletogenesis. *Development* **134**, 3917-3928.
Ambler, C. A., Nowicki, J. L., Burke, A. C. and Bautch, V. L. (2001). Assembly of trunk and limb blood vessels involves extensive migration and vasculogenesis of somite-derived angioblasts. *Dev. Biol.* **234**, 352-364.
Belteki, G., Haigh, J., Kabacs, N., Haigh, K., Sison, K., Costantini, F., Whitsett, J., Quaggin, S. E. and Nagy, A. (2005). Conditional and inducible transgene expression in mice through the combinatorial use of Cre-mediated recombination and tetracycline induction. *Nucleic Acids Res.* **33**, e51.
Benjamin, L. E., Hemo, I. and Keshet, E. (1998). A plasticity window for blood vessel remodelling is defined by pericyte coverage of the preformed endothelial network and is regulated by PDGF-B and VEGF. *Development* **125**, 1591-1598.
Carmeliet, P. (2000). Mechanisms of angiogenesis and arteriogenesis. *Nat. Med.* **6**, 389-395.
Chae, S. S., Paik, J. H., Allende, M. L., Proia, R. L. and Hla, T. (2004). Regulation of limb development by the sphingosine 1-phosphate receptor S1p1/EDG-1 occurs via the hypoxia/VEGF axis. *Dev. Biol.* **268**, 441-447.
Choi, J., Mouillesseaux, K., Wang, Z., Fiji, H. D., Kinderman, S. S., Otto, G. W., Geisler, R., Kwon, O. and Chen, J. N. (2011). Aplexone targets the HMG-CoA reductase pathway and differentially regulates arteriovenous angiogenesis. *Development* **138**, 1173-1181.
Coffin, J. D. and Poole, T. J. (1988). Embryonic vascular development: immunohistochemical identification of the origin and subsequent morphogenesis of the major vessel primordia in quail embryos. *Development* **102**, 735-748.
De Smet, F., Segura, I., De Bock, K., Hohensinner, P. J. and Carmeliet, P. (2009). Mechanisms of vessel branching: filopodia on endothelial tip cells lead the way. *Arterioscler. Thromb. Vasc. Biol.* **29**, 639-649.
Drake, C. J. and Little, C. D. (1999). VEGF and vascular fusion: implications for normal and pathological vessels. *J. Histochem. Cytochem.* **47**, 1351-1356.
Drake, C. J., Hungerford, J. E. and Little, C. D. (1998). Morphogenesis of the first blood vessels. *Ann. N. Y. Acad. Sci.* **857**, 155-719.
Eilken, H. M. and Adams, R. H. (2010). Dynamics of endothelial cell behavior in sprouting angiogenesis. *Curr. Opin. Cell Biol.* **22**, 617-625.
Eshkar-Oren, I., Viukov, S. V., Salameh, S., Krief, S., Oh, C. D., Akiyama, H., Gerber, H. P., Ferrara, N. and Zelzer, E. (2009). The forming limb skeleton serves as a signaling center for limb vasculature patterning via regulation of Vegf. *Development* **136**, 1263-1272.
Flamme, I., von Reutern, M., Drexler, H. C., Syed-Ali, S. and Risau, W. (1995). Overexpression of vascular endothelial growth factor in the avian embryo induces hypervascularization and increased vascular permeability without alterations of embryonic pattern formation. *Dev. Biol.* **171**, 399-414.
Folkman, J. (2003). Fundamental concepts of the angiogenic process. *Curr. Mol. Med.* **3**, 643-651.
Forsythe, J. A., Jiang, B. H., Iyer, N. V., Agani, F., Leung, S. W., Koos, R. D. and Semenza, G. L. (1996). Activation of vascular endothelial growth factor gene transcription by hypoxia-inducible factor 1. *Mol. Cell. Biol.* **16**, 4604-4613.
Gerber, H. P., Hillan, K. J., Ryan, A. M., Kowalski, J., Keller, G. A., Rangell, L., Wright, B. D., Radtke, F., Aguet, M. and Ferrara, N. (1999). VEGF is required for growth and survival in neonatal mice. *Development* **126**, 1149-1159.
Gerhardt, H. (2008). VEGF and endothelial guidance in angiogenic sprouting. *Organogenesis* **4**, 241-246.
Gerhardt, H., Golding, M., Fruttiger, M., Ruhrberg, C., Lundkvist, A., Abramsson, A., Jeltsch, M., Mitchell, C., Alitalo, K., Shima, D. et al. (2003). VEGF guides angiogenic sprouting utilizing endothelial tip cell filopodia. *J. Cell Biol.* **161**, 1163-1177.
Gossen, M., Freundlieb, S., Bender, G., Muller, G., Hillen, W. and Bujard, H. (1995). Transcriptional activation by tetracyclines in mammalian cells. *Science* **268**, 1766-1769.
Hellstrom, M., Phng, L. K., Hofmann, J. J., Wallgard, E., Coultas, L., Lindblom, P., Alva, J., Nilsson, A. K., Karlsson, L., Gaiano, N. et al. (2007). Dll4 signalling through Notch1 regulates formation of tip cells during angiogenesis. *Nature* **445**, 776-780.
Hla, T., Venkataraman, K. and Michaud, J. (2008). The vascular S1P gradient-cellular sources and biological significance. *Biochim. Biophys. Acta* **1781**, 477-482.
Hungerford, J. E. and Little, C. D. (1999). Developmental biology of the vascular smooth muscle cell: building a multilayered vessel wall. *J. Vasc. Res.* **36**, 2-27.
Isogai, S., Lawson, N. D., Torrealday, S., Horiguchi, M. and Weinstein, B. M. (2003). Angiogenic network formation in the developing vertebrate trunk. *Development* **130**, 5281-5290.
Jain, R. K. (2003). Molecular regulation of vessel maturation. *Nat. Med.* **9**, 685-693.
Jakobsson, L., Franco, C. A., Bentley, K., Collins, R. T., Ponsioen, B., Aspalter, I. M., Rosewell, I., Busse, M., Thurston, G., Medvinsky, A. et al. (2010). Endothelial cells dynamically compete for the tip cell position during angiogenic sprouting. *Nat. Cell Biol.* **12**, 943-953.
Kimmel, C. B., Ballard, W. W., Kimmel, S. R., Ullmann, B. and Schilling, T. F. (1995). Stages of embryonic development of the zebrafish. *Dev. Dyn.* **203**, 253-310.
Larrivee, B., Freitas, C., Suchting, S., Brunet, I. and Eichmann, A. (2009). Guidance of vascular development: lessons from the nervous system. *Circ. Res.* **104**, 428-441.
Lee, J. F., Ozaki, H., Zhan, X., Wang, E., Hla, T. and Lee, M. J. (2006). Sphingosine-1-phosphate signaling regulates lamellipodia localization of cortactin complexes in endothelial cells. *Histochem. Cell Biol.* **126**, 297-304.
Lee, M. J., Van Brocklyn, J. R., Thangada, S., Liu, C. H., Hand, A. R., Menzeleev, R., Spiegel, S. and Hla, T. (1998). Sphingosine-1-phosphate as a ligand for the G protein-coupled receptor EDG-1. *Science* **279**, 1552-1555.
Liu, Y., Cox, S. R., Morita, T. and Kourembanas, S. (1995). Hypoxia regulates vascular endothelial growth factor gene expression in endothelial cells. Identification of a 5′ enhancer. *Circ. Res.* **77**, 638-643.
Liu, Y., Wada, R., Yamashita, T., Mi, Y., Deng, C. X., Hobson, J. P., Rosenfeldt, H. M., Nava, V. E., Chae, S. S., Lee, M. J. et al. (2000). Edg-1, the G protein-coupled receptor for sphingosine-1-phosphate, is essential for vascular maturation. *J. Clin. Invest.* **106**, 951-961.
Lobov, I. B., Renard, R. A., Papadopoulos, N., Gale, N. W., Thurston, G., Yancopoulos, G. D. and Wiegand, S. J. (2007). Delta-like ligand 4 (Dll4) is

induced by VEGF as a negative regulator of angiogenic sprouting. *Proc. Natl. Acad. Sci. USA* **104**, 3219-3224.
Logan, M., Martin, J. F., Nagy, A., Lobe, C., Olson, E. N. and Tabin, C. J. (2002). Expression of Cre recombinase in the developing mouse limb bud driven by a Prxl enhancer. *Genesis* **33**, 77-80.
Meng, H. and Lee, V. M. (2009). Differential expression of sphingosine-1-phosphate receptors 1-5 in the developing nervous system. *Dev. Dyn.* **238**, 487-500.
Nehls, V. and Drenckhahn, D. (1993). The versatility of microvascular pericytes: from mesenchyme to smooth muscle? *Histochemistry* **99**, 1-12.
Paik, J. H., Skoura, A., Chae, S. S., Cowan, A. E., Han, D. K., Proia, R. L. and Hla, T. (2004). Sphingosine 1-phosphate receptor regulation of N-cadherin mediates vascular stabilization. *Genes Dev.* **18**, 2392-2403.
Pappu, R., Schwab, S. R., Cornelissen, I., Pereira, J. P., Regard, J. B., Xu, Y., Camerer, E., Zheng, Y. W., Huang, Y., Cyster, J. G. et al. (2007). Promotion of lymphocyte egress into blood and lymph by distinct sources of sphingosine-1-phosphate. *Science* **316**, 295-298.
Potente, M., Gerhardt, H. and Carmeliet, P. (2011). Basic and therapeutic aspects of angiogenesis. *Cell* **146**, 873-887.
Risau, W. (1991). Embryonic angiogenesis factors. *Pharmacol. Ther.* **51**, 371-376.
Risau, W. (1997). Mechanisms of angiogenesis. *Nature* **386**, 671-674.
Risau, W. and Flamme, I. (1995). Vasculogenesis. *Annu. Rev. Cell Dev. Biol.* **11**, 73-91.
Ruhrberg, C., Gerhardt, H., Golding, M., Watson, R., Ioannidou, S., Fujisawa, H., Betsholtz, C. and Shima, D. T. (2002). Spatially restricted patterning cues provided by heparin-binding VEGF-A control blood vessel branching morphogenesis. *Genes Dev.* **16**, 2684-2698.
Ryan, H. E., Poloni, M., McNulty, W., Elson, D., Gassmann, M., Arbeit, J. M. and Johnson, R. S. (2000). Hypoxia-inducible factor-1alpha is a positive factor in solid tumor growth. *Cancer Res.* **60**, 4010-4015.
Santoro, M. M., Pesce, G. and Stainier, D. Y. (2009). Characterization of vascular mural cells during zebrafish development. *Mech. Dev.* **126**, 638-649.
Schmid, G., Guba, M., Ischenko, I., Papyan, A., Joka, M., Schrepfer, S., Bruns, C. J., Jauch, K. W., Heeschen, C. and Graeb, C. (2007). The immunosuppressant FTY720 inhibits tumor angiogenesis via the sphingosine 1-phosphate receptor 1. *J. Cell. Biochem.* **101**, 259-270.
Seichert, V. and Rychter, Z. (1972a). Vascularization of developing anterior lamb of the chick embryo. II. Differentiation of vascular bed and its significance for the location of morphogenetic processes inside the limb bud. *Folia Morphol. (Praha)* **20**, 352-361.
Seichert, V. and Rychter, Z. (1972b). Vascularization of the developing anterior limb of the chick embryo. 3. Developmental changes in the perimetacarpal capillary network. *Folia Morphol. (Praha)* **20**, 397-405.
Serbedzija, G. N., Flynn, E. and Willett, C. E. (1999). Zebrafish angiogenesis: a new model for drug screening. *Angiogenesis* **3**, 353-359.
Suchting, S., Freitas, C., le, Noble, F., Benedito, R., Breant, C., Duarte, A. and Eichmann, A. (2007). The Notch ligand Delta-like 4 negatively regulates endothelial tip cell formation and vessel branching. *Proc. Natl. Acad. Sci. USA* **104**, 3225-3230.
Thisse, C. and Thisse, B. (2008). High-resolution in situ hybridization to whole-mount zebrafish embryos. *Nat. Protoc.* **3**, 59-69.
Vargesson, N. and Laufer, E. (2001). Smad7 misexpression during embryonic angiogenesis causes vascular dilation and malformations independently of vascular smooth muscle cell function. *Dev. Biol.* **240**, 499-516.
Venkataraman, K., Lee, Y. M., Michaud, J., Thangada, S., Ai, Y., Bonkovsky, H. L., Parikh, N. S., Habrukowich, C. and Hla, T. (2008). Vascular endothelium as a contributor of plasma sphingosine 1-phosphate. *Circ. Res.* **102**, 669-676.
von Tell, D., Armulik, A. and Betsholtz, C. (2006). Pericytes and vascular stability. *Exp. Cell Res.* **312**, 623-629.
Weinstein, B. M. (2005). Vessels and nerves: marching to the same tune. *Cell* **120**, 299-302.
Wiley, D. M., Kim, J. D., Hao, J., Hong, C. C., Bautch, V. L. and Jin, S. W. (2011). Distinct signalling pathways regulate sprouting angiogenesis from the dorsal aorta and the axial vein. *Nat. Cell Biol.* **13**, 686-692.
Yaniv, K., Isogai, S., Castranova, D., Dye, L., Hitomi, J. and Weinstein, B. M. (2006). Live imaging of lymphatic development in the zebrafish. *Nat. Med.* **12**, 711-716.
Yatomi, Y., Ohmori, T., Rile, G., Kazama, F., Okamoto, H., Sano, T., Satoh, K., Kume, S., Tigyi, G., Igarashi, Y. et al. (2000). Sphingosine 1-phosphate as a major bioactive lysophospholipid that is released from platelets and interacts with endothelial cells. *Blood* **96**, 3431-3438.
Yonesu, K., Kawase, Y., Inoue, T., Takagi, N., Tsuchida, J., Takuwa, Y., Kumakura, S. and Nara, F. (2009). Involvement of sphingosine-1-phosphate and S1P1 in angiogenesis: analyses using a new S1P1 antagonist of non-sphingosine-1-phosphate analog. *Biochem. Pharmacol.* **77**, 1011-1020.
Zhong, T. P. (2005). Zebrafish genetics and formation of embryonic vasculature. *Curr. Top. Dev. Biol.* **71**, 53-81.

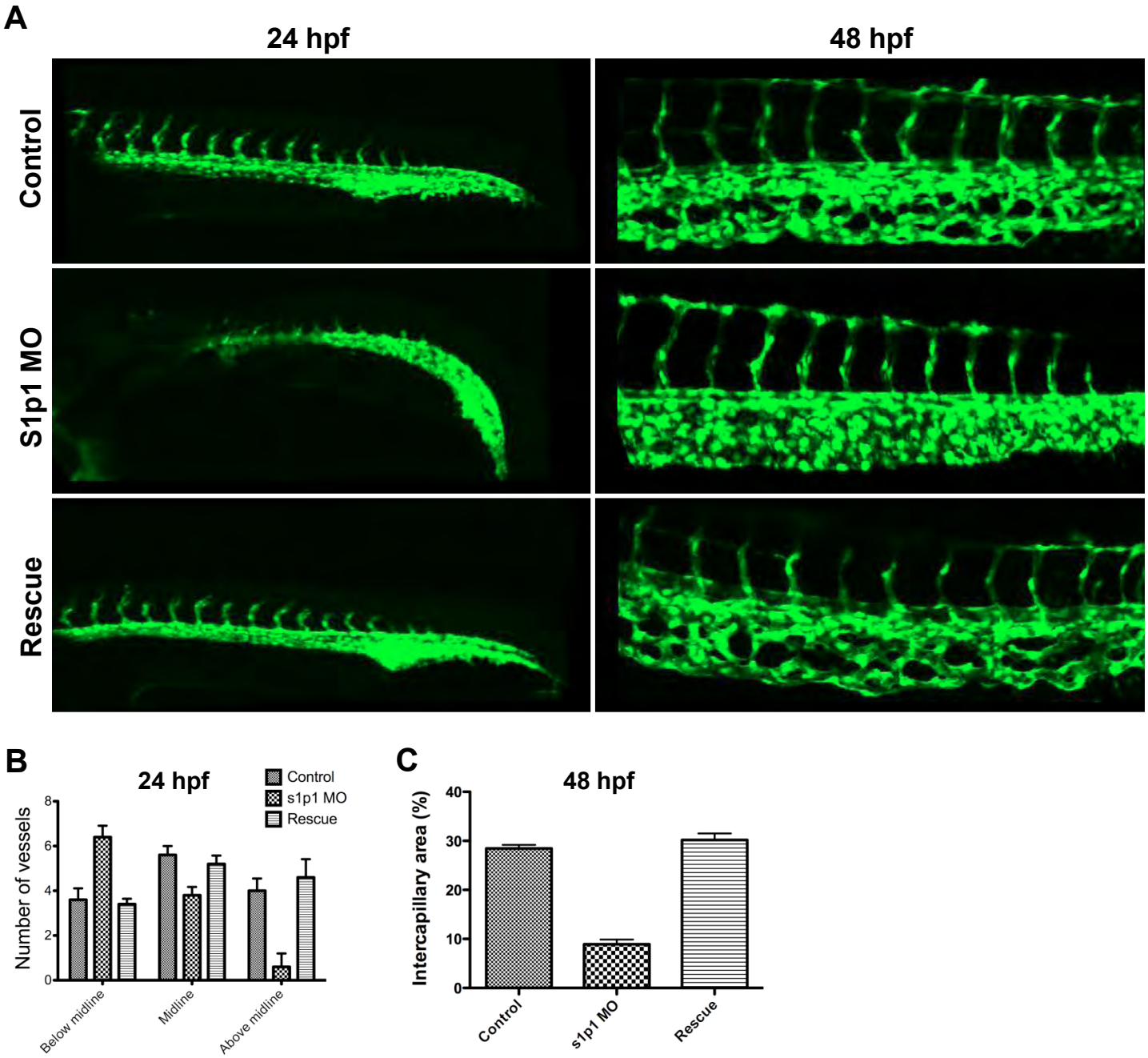

Fig. S1. Rescue of the vascular phenotype by *s1p1* mRNA injection. (**A**) Fluorescence microscope images of control (upper panel), *s1p*$_1$ MO (middle) and *s1p1* mRNA-injected morphant (lower panel) zebrafish embryos at 24 (left) and 48 hpf (right). (**B**) Quantification of ISV location relative to the midline. Both mRNA-injected (rescue experiment) and non-injected *s1p*$_1$ MO zebrafish were compared with control embryos (n=6 WT, 6 MO and 6 mRNA-injected embryos, 6-8 ISVs from each embryo were analyzed; *s1p*$_1$ MO: P<0.05; rescue experiment: $P_{\text{below midline}}$=0.74, P_{midline}=0.65, $P_{\text{above midline}}$=0.74; error bars represent s.e.m.). (**C**) Comparison of the intercapillary area in the CVP between WT, *s1p*$_1$ MO and mRNA-injected zebrafish (n=6 in all groups; $P_{\text{s1p1 MO}}$=0.002, P_{Rescue}=0.39, error bars represent s.e.m.).

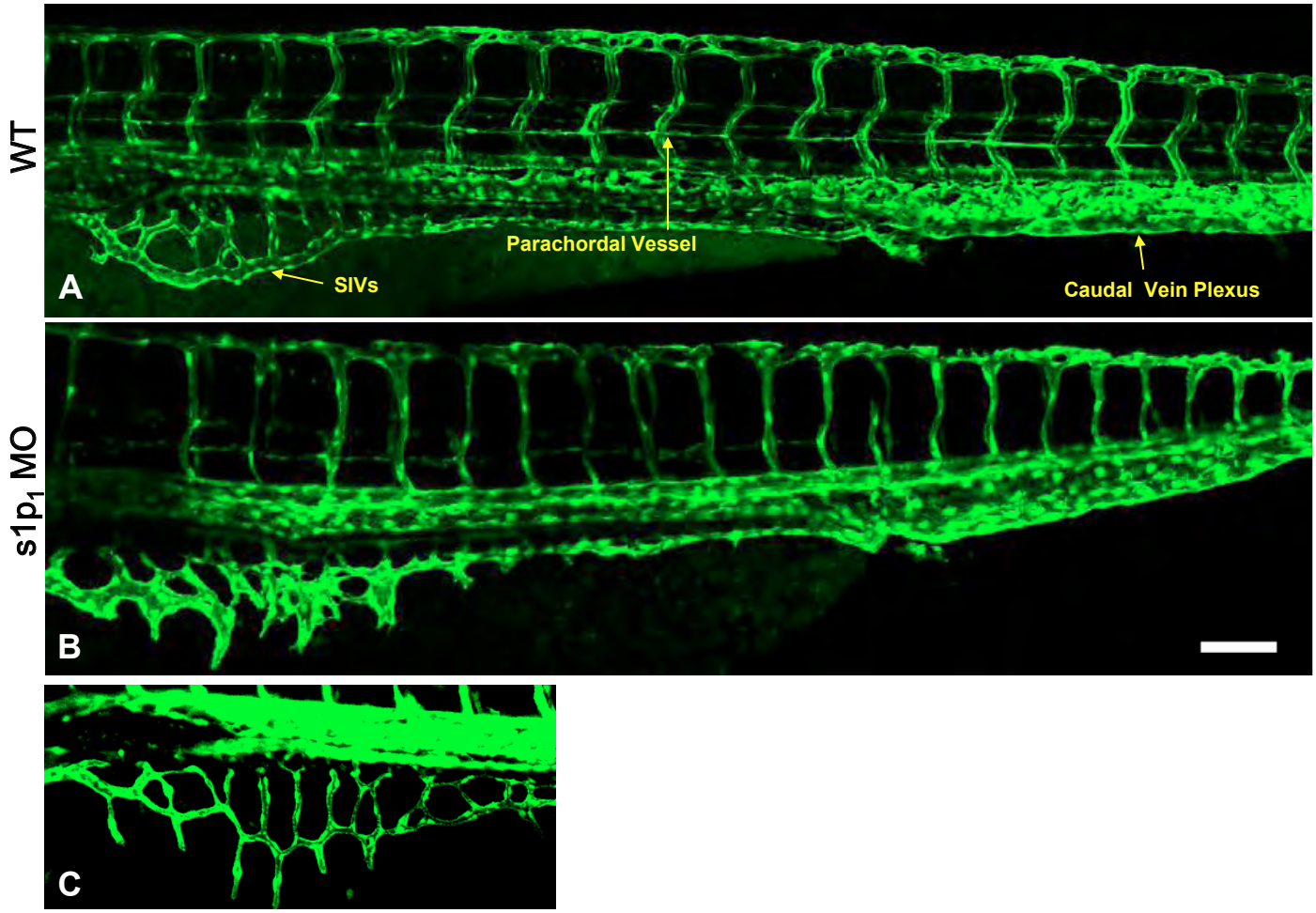

Fig. S2. S1p$_1$ knockdown in zebrafish causes defects in blood vessel formation. (**A-C**) Fluorescence microscopy of control (A) and *s1p$_1$* MO (B,C) embryos at 3 dpf. Arrows indicate subintestinal vessel (SIV), parachordal vein and caudal vein plexus. SIVs in the *s1p$_1$* MO embryo exhibit two phenotypes, namely dilated vessels (B) and ectopic sprouting (C). Scale bar: 100 μm.